PCCP

Accepted Manuscript

This is an *Accepted Manuscript*, which has been through the Royal Society of Chemistry peer review process and has been accepted for publication.

Accepted Manuscripts are published online shortly after acceptance, before technical editing, formatting and proof reading. Using this free service, authors can make their results available to the community, in citable form, before we publish the edited article. We will replace this *Accepted Manuscript* with the edited and formatted *Advance Article* as soon as it is available.

You can find more information about *Accepted Manuscripts* in the Information for Authors.

Please note that technical editing may introduce minor changes to the text and/or graphics, which may alter content. The journal's standard Terms & Conditions and the Ethical guidelines still apply. In no event shall the Royal Society of Chemistry be held responsible for any errors or omissions in this *Accepted Manuscript* or any consequences arising from the use of any information it contains.

ROYAL SOCIETY OF CHEMISTRY

www.rsc.org/pccp

PCCP

RSCPublishing

PAPER

On the possible biological relevance of HSNO isomers: A computational investigation

Cite this: DOI: 10.1039/xoxxoooooox

Lena V. Ivanova,[a] Becka J. Anton,[b,a] and Qadir K. Timerghazin*[a]

Received ooth January 2014,
Accepted ooth January 2014

DOI: 10.1039/xoxxoooooox

www.rsc.org/

Thionitrous acid HSNO, the smallest *S*-nitrosothiol, has been identified as a potential biologically active molecule that connects the biochemistries of two important gasotransmitters, nitric oxide NO and hydrogen sulfide H_2S. Here, we computationally explore possible isomerization reactions of HSNO that may occur at physiological conditions using high-level coupled-cluster as well as density functional theory and composite CBS-QB3 methodology calculations. Gas-phase calculations show that formation of the tautomeric form HONS and the *Y*-isomer SN(H)O is thermodynamically feasible, as they are energetically close, within ~6 kcal/mol, to HSNO, while the recently proposed three-membered ring isomer is not thermodynamically or kinetically accessible. Although the gas-phase intramolecular proton-transfer reactions required for HSNO isomerization into HONS and SN(H)O are predicted to have prohibitively high, 30–50 kcal/mol, reaction barriers, polar aqueous environment and assistance by water molecules should decrease these barriers to ~9 kcal/mol, which makes these two isomers kinetically accessible at physiological conditions. Our calculations also support a possibility of an aqueous reaction between the *Y*-isomer SN(H)O and H_2S leading to biologically active nitroxyl HNO. These results suggest that formation of HSNO in biological milieu can lead to various derivative species with their own, possibly biologically relevant, activity.

1. Introduction

S-nitrosothiols (RSNOs)—usually in the form of *S*-nitrosated cysteine residues—play an important biological role being involved in the storage and transport of nitric oxide NO as well as in exerting its regulatory function via protein *S*-nitrosation.[1-8] Until very recently, the smallest RSNO molecule— thionitrous acid HSNO—has not been considered as biologically relevant species, although it has been observed experimentally as a photolysis product of its isomer, HNSO, in argon matrix.[9-13] However, recent studies have shown that HSNO could form at physiologically relevant conditions and may act as an important intermediate in NO-related biochemical processes.[14-16] It has been proposed that HSNO could form in reactions between hydrogen sulfide H_2S and cysteine-based RSNOs, thereby connecting biochemistries of the two important biological messengers, H_2S and NO.[13,15,17,18] If HSNO indeed formed in biological milieu, its subsequent reactions may lead to other potentially bioactive small molecules or reactive intermediates.[13,17,19] For instance, King[17] has recently hypothesized that cyclic three-membered ring isomer of HSNO, further referred to as *cycl*-SONH, could be produced from HSNO in a stepwise process through HONS tautomer (Scheme 1A).

This cyclic isomer could then undergo a reaction with H_2S producing hydrogen disulfide HSSH and HNO (Scheme 1B). Thus, *cycl*-SONH may possibly be involved in formation of the elusive endogenous nitroxyl, HNO/NO^-, a potent signaling molecule of great pharmacological potential.[20-22] Unfortunately, this intriguing hypothesis is hard to verify experimentally, as *cycl*-SONH and HONS should be difficult to detect. In this respect, accurate electronic structure calculations can help to assess the likelihood of these HSNO isomers forming at physiological conditions.

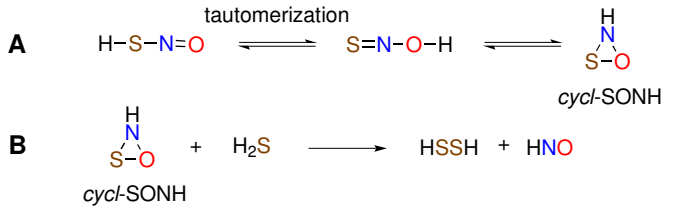

Scheme 1 Proposed[17] HSNO isomerization into a cyclic three-membered ring isomer *cycl*-SONH (A) and its subsequent reaction with hydrogen sulfide.

Reliable *ab initio* calculations of HSNO, and RSNOs in general, are challenging, as their geometry and energetic properties are highly dependent on the method and the basis set used.[23,24] Among *ab initio* methods, coupled cluster method including single, double, and triple excitations, CCSD(T), appears to be the lowest level of theory able to properly describe RSNOs.[24,25] The S–N bond properties are particularly sensitive

Physical Chemistry Chemical Physics Accepted Manuscript

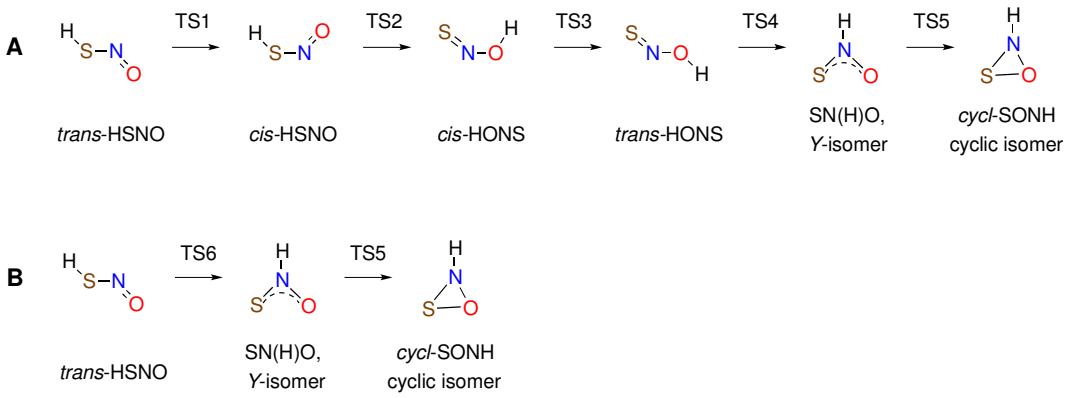

Scheme 2 Calculated HSNO isomerization pathways leading to the cyclic isomer *cycl*-SONH.

to the level of the electron correlation treatment, which is indicative of a multireference character of the –SNO group.[24,26] We have previously reported accurate *ab initio* calculations of HSNO at the CCSD(T) level corrected for the effect of quadruple excitations and extrapolated to the complete basis set limit (CBS), with corrections for core-valence electron correlation and relativistic effects.[24] On the other hand, computational investigations of HSNO isomers and their interconversion reactions reported in the literature have been performed less systematically and at lower levels of theory.[27-29] Moreover, HSNO isomerization reaction transition states (TSs) and corresponding barriers calculated in the gas phase may not be relevant for the aqueous biological environment, where they are likely to proceed via water-assisted proton transfer mechanism that significantly decreases reaction barriers. However, no water-assisted HSNO isomerization reaction studies have been reported so far, to the best of our knowledge.

Here, we report a computational investigation of the possible pathways of formation of the three-membered cyclic isomer *cycl*-SONH from HSNO using high-level *ab initio* coupled cluster calculations as well as hybrid density functional theory (DFT) and composite CBS-QB3 approaches. First, we use high-level coupled-cluster calculations at the CCSD(T) level extrapolated to the complete basis set limit and corrected for the effect of quadruple excitations to examine HSNO transformation pathways in the gas phase. High-level reference parameters for HSNO geometry and the S–N bond dissociation energy reported previously[24] have also been updated with improved correction for the effect of quadruple excitations in the coupled cluster expansion as well as an improved ZPE correction (Figure 1). The coupled-cluster reference data have been used to validate less computationally expensive CBS-QB3 and DFT methods. These methods have been used to investigate the effect of aqueous environment on HSNO isomerization reactions, and to study the feasibility of HNO formation in the reactions of HSNO isomers with hydrogen sulfide.

2. Computational details

Ab initio electronic structure calculations were performed with the Molpro 2010.1 package[30] using coupled cluster method with single double and perturbative triple excitations CCSD(T).[31,32] The CCSD(T) results were further improved with coupled cluster calculations with single, double, triple, and perturbative quadruple excitations, CCSDT(Q),[33] performed using MRCC[34] code interfaced with CFOUR program.[35] Standard T_1 and D_1 diagnostics[36,37] were used to estimate the quality of single-reference description of the wavefunction. Molecular geometry optimizations were performed at the CCSD(T) level using numerical gradients. As these calculations are time consuming and require significant computational power, the geometry optimizations were performed using DL-FIND[38] code using in-house interface with Molpro and CFOUR to split the numerical gradient calculations across the nodes of a computational cluster. Geometries were optimized with L-BFGS[39,40] method in Cartesian coordinates and transition states were found with the partitioned rational functional optimization (P-RFO)[41-44] using delocalized internal coordinates (DLC) with total connections (TC).[45] The convergence criteria were 4.5×10^{-5} and 1.0×10^{-6} for the component of gradient and energy change respectively.

A series of Dunning's augmented correlation consistent basis sets,[46] aug-cc-pV*x*Z (*x* = D, T, Q and 5) were used for all elements except sulfur, for which basis sets with additional tight *d*-functions, aug-cc-pV(*x*+*d*)Z were employed,[47] a combination abbreviated as AV*x*Z. Molecular geometries were optimized at the frozen-core CCSD(T) level with AVDZ, AVTZ, AVQZ and AV5Z basis sets. Transition state geometries were optimized at CCSD(T) level with AVDZ, AVTZ and AVQZ basis sets, and single-point energy calculations were performed with AV5Z basis set for AVQZ geometries. Extrapolations to the complete basis set (CBS) of the energy and molecular geometry were employed using three slightly different schemes.

The first, most accurate extrapolation scheme used, $CBS_{TQ5/Q5}$, form hereon referred to as simply CBS, was applied

Physical Chemistry Chemical Physics Accepted Manuscript

 This journal is © the Owner Societies 2014

to molecular geometries and their energetic properties. It uses an average of the mixed Gaussian/exponential formula[48,49]

$$E(n) = b_{CBS} + \frac{B}{n^3}$$

for AVTZ, AVQZ and AV5Z basis sets (n = 3, 4, 5), and the two-parameter extrapolation formula[50]

$$E(n) = b_{CBS} + Be^{(-(n-1))} + Ce^{(-(n-1)^2)}$$

for AVQZ and AV5Z (n =4, 5). As the transition state (TS) calculations are generally more difficult, TS geometry optimizations were done only up to the AVQZ basis set. In this case, two-parameter extrapolation using AVTZ and AVQZ basis sets, CBS_{TQ}, was used for geometries and energies. Also, the two-parameter extrapolation was applied to AVQZ and single-point AV5Z energies calculated for AVQZ-optimized geometries, denoted as CBS_{Q5sp}.

The effect of inclusion of quadruple excitation in the coupled cluster calculations ΔQ was estimated at the frozen core CCSDT(Q) level as a difference between the results obtained with CCSDT(Q)/cc-pVDZ and CCSD(T)/cc-pVDZ geometry optimizations.

Corrections for the scalar-relativistic effects ΔSR were estimated with the Douglas-Kroll-Hess[51,52] approach using the cc-VQZ_DK[30] basis set as a difference between the values obtained from geometry optimizations at CCSD(T)/cc-VQZ_DK with and without the inclusion of SR effects. Core-valence correlation corrections ΔCV were estimated at the CCSD(T) level using weighted CV basis set, aug-cc-pwCVQZ,[53] for geometries optimized at CCSD(T)/aug-pwCVTZ level as a difference between the values obtained with full-electron correlation (excluding sulfur 1s electrons) and those from frozen-core calculations. Zero-point vibrational energies (ZPEs) were calculated from CCSD(T)/AVQZ harmonic vibrational frequencies evaluated numerically.

As one of the TSs calculated here (**TS5**) has been found to have a significant open-shell character, its geometry along with the corresponding product and reagent, were optimized with second-order multireference perturbation theory (CASPT2)[54] method as implemented in Molpro.[30] The reference complete active space self-consistent field (CASSCF)[55,56] wavefunction used '6 electrons in 6 orbitals' (6,6) active space, chosen from the analysis of the natural orbitals from the second-order perturbation theory calculation with RHF reference for the TS structure. CASPT2 geometry optimizations were performed using AVDZ, AVTZ, AVQZ and AV5Z basis sets with analytical gradients.[57] Zero-point vibrational energies (ZPEs) were calculated from CASPT2/AVQZ harmonic vibrational frequencies in the Molpro.[30] Single point multireference configuration interaction with Davidson correction[55,56,58] (MRCI+Q) calculation with AVQZ basis set was applied for geometries optimized at the CASPT2/AVQZ.

Density functional theory (DFT) calculations with Perdew-Burke-Ernzenhof hybrid functional (PBE0) method,[59,60] as well as calculations using a composite CBS-QB3 methodology[61] were performed with Gaussian 09 package.[62] PBE0 calculations used a polarized triple-zeta basis set by Weigend and Ahlrichs[63] with diffuse functions by Rapport and Furche,[64] def2-TZVPPD. The chemical nature of all transition states obtained with PBE0 and CBS-QB3 was confirmed by the intrinsic reaction coordinate (IRC) reaction path calculations.[65,66] Solvent effects were included using the implicit integral equation formalism polarizable continuum model (IEF-PCM).[67]

3. Results and discussion

Our calculations show that the reaction pathway of HSNO isomerization into the cyclic form, *cycl*-SONH, is more complicated (Scheme 2A) than previously proposed (Scheme 1A): it requires transformations between *trans*- and *cis*- conformers of HSNO and HONS and proceeds via additional intermediate, SN(H)O or the *Y*-isomer. Besides this pathway, which involves six isomers and five TSs, we found a shorter, two-step pathway (Scheme 2B) for the *trans*-HSNO transformation into *cycl*-SONH via the *Y*-isomer only.

Figure 2 shows the energy profiles for the two possible pathways of *trans*-HSNO conversion into *cycl*-SONH, computed at the coupled-cluster level, along with the structures of relevant of HSNO isomers and transition states (TSs). While the structures of HSNO isomers were optimized with the basis sets up to AV5Z that allowed accurate CBS extrapolations of the energetic and geometric parameters, which are reported at the CCSD(T)/CBS+CORR, CORR=ΔQ+ΔCV+ΔSR level, with the energies also corrected for the zero-point vibrational energy, ZPE. As the TS structures are difficult to optimize, the reported TS geometries and the reaction barriers are based on slightly less accurate CBS_{TQ} and CBS_{Q5sp} extrapolation schemes. In the most computationally challenging case of the HSNO molecule and its *trans*-to-*cis* isomerization barrier the CBS_{Q5sp} results are within 0.1 kcal/mol and the bond lengths obtained with CBS_{TQ} are within 0.003 Å of the full CBS values. For consistency, the energies and geometries shown in Figure 2 are based on the CCSD(T)/CBS_{Q5sp}+CORR+ZPE and CCSD(T)/CBS_{TQ}+CORR results, respectively. Tables 1–3 list the geometries and energies (relative to *trans*-HSNO) of HSNO conformers and isomers obtained at various levels of theory, and Table S1 in Supporting Information lists all the data regarding the calculated reaction barriers.

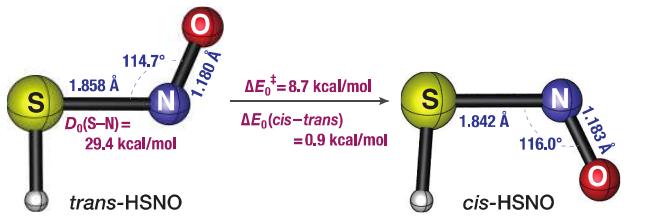

Physical Chemistry Chemical Physics Accepted Manuscript

Figure 1 Recommended geometric and energetic parameters of HSNO estimated at the CCSD(T)/CBS level with corrections for quadruple excitations, core-valence correlation, relativistic effects, and zero-point vibrational energy (ZPE, for energetic parameters). Earlier results in Ref. 24 have been updated with improved correction for quadruple excitations and improved ZPE values, as detailed in the text.

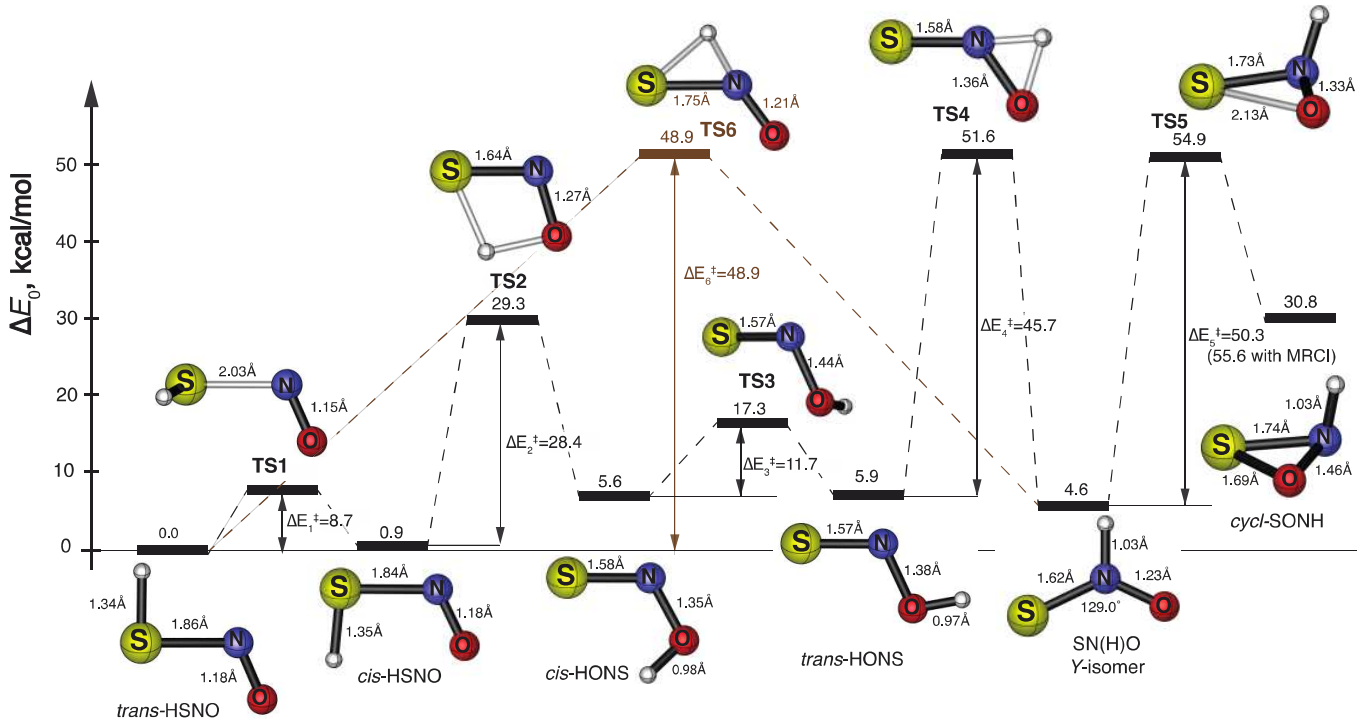

Figure 2 Energetic profiles for the two reactions pathways of HSNO isomerization into the cyclic isomer *cycl*-SONH (Scheme 2). Energetic parameters calculated at the CCSD(T)/CBS_{Q5sp}+CORR+ZPE level, except **TS5** which is calculated at the CCSD(T)/CBS_{TQ}+CORR+ZPE level.[68] Molecular and TS geometries are obtained at the CCSD(T)/CBS_{TQ}+CORR+ZPE level.

3.1 HSNO: Improved coupled-cluster description

Previously,[24] we reported a high-level *ab initio* coupled-cluster investigation of HSNO that highlighted the slow convergence of the S–N bond properties with respect to the single-electron basis set size and the level of electron correlation treatment. For instance, coupled cluster calculations with only single and double excitations included (CCSD) were found highly unreliable, as they underestimate the S–N bond length by >0.05 Å and its bond dissociation energy by >6 kcal/mol. Even the "gold standard" CCSD(T) method is not sufficient for accurate quantitative description of HSNO, as it requires a correction for the effect of computationally expensive quadruple excitations in the coupled-cluster expansion. In the earlier work,[24] we estimated the effects of quadruple excitations at the CCSDT(Q) level using a smaller VDZ basis set by Ahlrichs and partial geometry optimization with only the S–N bond relaxed. Here, we improve upon these calculations by fully relaxed geometry optimizations of the two HSNO conformers at the CCSDT(Q) level with larger, fully polarized cc-pVDZ basis set, which suggest even larger effect of quadruples on the S–N bond length and dissociation energy, 0.03 Å and 1.3 kcal/mol vs earlier estimations of 0.02 Å and 1 kcal/mol, respectively. Tables 1 and S1 (in Supplementary Information) summarize the calculated geometric parameters of HSNO; the final recommended S–N lengths in *trans*- and *cis*-HSNO are 1.858 Å and 1.842 Å, respectively, evaluated at the CCSD(T)/CBS+CORR level (Figure 2).

The calculated energetic properties of HSNO were also improved in this work by using harmonic ZPE correction obtained at the CCSD(T)/AVQZ level, whereas the earlier work used a smaller AVTZ basis set. The recommended value for the energy of *cis*-HSNO relative to the more stable *trans*-form is 8.69 kcal/mol at the CCSD(T)/CBS+CORR+ZPE level. The final recommended S–N bond dissociation energy is 29.4 kcal/mol (Figure 2), calculated at the CCSD(T)/CBS+CORR+SO+ZPE level, which also includes a spin-orbit (SO) energy correction[24] for the HS˙ radical.

We also calculated TS for *trans*-to-*cis* isomerization (Table 1, **TS1** in Figure 2); it is characterized by 345*i* cm^{-1} imaginary frequency, and has a nearly perpendicular geometry and a highly elongated S–N bond, ~0.18 Å longer than in *trans*-HSNO. Like in the case of the equilibrium HSNO structures, the calculated S–N bond length in the TS decreases with the basis set size, from 2.067 Å with AVDZ to 2.015 Å with AV5Z, and significantly increases (~0.025 Å) when a correction for quadruple excitations is included. The corresponding barrier height increases with the basis set size, form 8.08 kcal/mol with AVDZ to 8.93 kcal/mol with AV5Z, and the inclusion of quad-

Physical Chemistry Chemical Physics Accepted Manuscript

 This journal is © the Owner Societies 2014

ruple excitations further increases it by 0.5 kcal/mol. Harmonic ZPE correction decreases the barrier by 0.8 kcal/mol. The final estimation for the *trans*-to-*cis* isomerization barrier is 8.7 kcal/mol at the CCSD(T)/CBS+CORR+ZPE level (Table 1).

Table 1 Geometric parameters of *trans*- and *cis*-HSNO, energy difference between them, geometric parameters of the TS for their interconversion, and the corresponding barrier height ($\Delta E_1^{\ddagger}$, kcal/mol), calculated at different levels of theory.

	trans-HSNO			*cis*-HSNO				**TS1**				
	S–N/Å	N–O/Å	SNO/°	S–N/Å	N–O/Å	SNO/°	$E_{cis\text{-HSNO}}$	S–N/Å	N–O/Å	SNO/°	ONSH/°	$\Delta E_1^{\ddagger}$
CCSD(T)/												
AVDZ	1.903	1.189	114.50	1.894	1.192	115.49	1.05	2.067	1.171	112.92	87.63	8.08
AVTZ	1.860	1.183	114.55	1.847	1.187	115.76	0.97	2.031	1.161	112.99	87.48	8.62
AVQZ	1.846	1.181	114.54	1.830	1.184	115.88	0.93	2.019	1.158	113.00	87.51	8.85
AV5Z	1.841	1.181	114.50	1.825	1.184	115.87	0.91	2.015	1.157	112.95	87.51	8.93
CBS	1.837	1.181	114.47	1.821	1.184	115.86	0.90	2.012	1.157	112.91	87.51	8.99
CBS_{TQ}	1.836	1.180	114.53	1.818	1.182	115.97	0.91	2.010	1.156	113.01	87.53	9.02
CBS_{Q5sp}							0.89					9.00
ΔQ	0.033	-0.001	0.34	0.034	-0.001	0.04	0.10	0.025	0.000	0.03	0.45	0.54
ΔCV	-0.007	-0.001	0.01	-0.008	-0.001	0.07	-0.01	-0.007	-0.001	0.02	-0.02	0.11
ΔSR	-0.005	0.001	-0.07	-0.005	0.001	-0.04	0.00	0.006	-0.001	-0.03	0.08	-0.09
ΔZPE							-0.10					-0.83
CBS+CORR	1.858	1.180	114.74	1.842	1.183	115.93	1.00	2.035	1.155	112.94	88.02	9.52
CBS+CORR+ZPE							0.90					8.69
CBS_{TQ}+CORR	1.856	1.179	114.81	1.839	1.181	116.04	1.00	2.034	1.154	113.04	88.05	9.57
CBS_{TQ}+CORR+ZPE							0.91					8.74
CBS_{5sp}+CORR+ZPE							0.89					8.72
PBE0/def2-TZVPPD	1.828	1.167	115.31	1.811	1.170	116.95	1.07	1.983	1.144	113.59	87.89	11.06
PBE0/def2-TZVPPD+ZPE							0.88					10.25
CBS-QB3	1.929	1.163	115.27	1.917	1.165	116.24	1.13	2.082	1.145	113.35	87.87	8.66
CBS-QB3+ZPE							0.99					7.91

Compared to the full CBS scheme, less computationally expensive CBS_{Q5sp} extrapolation gives the energies within 0.03 kcal/mol while the CBS_{TQ} extrapolated bond lengths are within 0.003 Å. DFT calculations with PBE0 functional as well as calculations with CBS-QB3 composite methodology reproduce the high-level results reasonably well. The S–N bond optimized at PBE0 method is underestimated by 0.03 Å for *trans*-HSNO and *cis*-HSNO, by 0.05 Å for the TS. This method overestimates the *trans*-to-*cis* interconversion barrier by 1.5 kcal/mol, 10.3 kcal/mol vs 8.7 kcal/mol at the CCSD(T)/CBS+CORR+ZPE. However, the energy difference between *cis*- and *trans*-forms is almost the same, 0.9 kcal/mol (Figure 2, Table 1). CBS-QB3 methodology, which employs B3LYP/6-311G(*2d,d,p*) DFT method for geometry optimization, overestimates the S–N bond by 0.05 Å for transition state, by 0.07 Å for *trans*-HSNO and *cis*-HSNO. *Trans*-to-*cis* interconversion barrier is underestimated by 0.8 kcal/mol (7.9 kcal/mol), while the energy difference between *cis*- and *trans*-forms is overestimated by 0.1 kcal/mol (1.0 kcal/mol).

3.2 HONS, the tautomeric form

HONS, the tautomeric form of HSNO, also exists as nearly isoenergetic *trans*- and *cis*- conformers (Figure 2). Slightly more stable cis-HONS is 5.6 kcal/mol higher in energy relative

Physical Chemistry Chemical Physics Accepted Manuscript

to *trans*-HSNO, whereas *trans*-HONS is just 0.3 kcal/mol less stable (Table 2, Figure 2). The TS for *cis*-to-*trans* isomerization is slightly higher than for the similar transformation of HSNO:

Table 2 Geometric parameters of *cis*- and *trans*-HONS, their energy relative to *trans*-HSNO (ΔE, kcal/mol), geometric parameters of the TS for their interconversion, and the corresponding barrier height ($\Delta E_3^{\ddagger}$, kcal/mol) calculated at different levels of theory.

	cis-HONS				*trans*-HONS				**TS3**				
	S–N/Å	N–O/Å	SNO/°	ΔE	S–N/Å	N–O/Å	SNO/°	ΔE	S–N/Å	N–O/Å	SNO/°	HONS/°	$\Delta E_3^{\ddagger}$
CCSD(T)/													
AVDZ	1.608	1.374	115.85	5.51	1.597	1.403	112.42	5.55	1.591	1.468	112.78	86.77	11.95
AVTZ	1.591	1.361	115.99	3.62	1.581	1.389	112.85	3.75	1.574	1.450	113.13	87.00	12.23
AVQZ	1.585	1.355	116.11	3.23	1.575	1.382	113.04	3.49	1.568	1.441	113.31	87.15	12.56
AV5Z	1.582	1.353	116.12	3.07	1.573	1.380	113.10	3.35					
CBS	1.580	1.352	116.13	2.98	1.571	1.379	113.15	3.27					
CBS_{TQ}	1.580	1.350	116.19	2.95	1.571	1.376	113.18	3.29	1.564	1.435	113.43	87.27	12.80
CBS_{Q5sp}				2.91				3.21					12.65
ΔQ	0.003	0.003	-0.12	0.93	0.003	0.005	-0.12	0.89	0.003	0.003	-0.03	0.15	0.17
ΔCV	-0.004	-0.003	0.07	-0.12	-0.004	-0.003	0.69	-0.14	-0.003	-0.003	0.07	-0.01	0.04
ΔSR	0.001	0.000	-0.01	-0.29	0.001	0.001	-0.08	-0.29	0.001	0.001	-0.06	-0.03	-0.04
ΔZPE				2.21				2.26					-1.16
CBS+ CORR	1.581	1.353	116.06	3.50	1.571	1.382	113.63	3.74					
CBS+CORR+ZPE				5.71				6.00					
CBS_{TQ}+ CORR	1.581	1.350	116.13	3.48	1.571	1.378	113.66	3.76	1.565	1.435	113.42	87.38	12.96
CBS_{TQ}+CORR+ZPE				5.68				6.02					11.80
CBS_{5sp}+CORR+ZPE				5.64				5.94					11.65
PBE0/													
def2-TZVPPD	1.571	1.325	117.16	5.35	1.562	1.352	114.30	6.18	1.552	1.409	114.50	88.31	15.26
def2-TZVPPD+ZPE				7.55				8.48					14.05
CBS-QB3	1.585	1.340	116.87	2.93	1.573	1.378	113.92	2.94	1.563	1.434	114.03	87.94	12.31
CBS-QB3+ZPE				5.11				5.21					11.09

11.7 kcal/mol vs 8.7 kcal/mol, respectively. Overall, the calculated HONS properties demonstrate much more robust convergence with respect to the basis set size and electron correlation treatment. Interestingly, compared to the other bonds in HONS, the O–N bond length still demonstrates the slowest convergence with the basis set and the largest ΔQ correction (~0.005 Å). Also, somewhat reminiscent to the S–N bond in HSNO, this bond O–N bond demonstrates significant elongation in the *cis*-to-*trans* isomerization TS (~0.09 Å).

Compared against the high-level coupled-cluster data, CBS-QB3 methodology reproduces the energetic and geometric parameters of HONS and its *cis*-to-*trans* isomerization TS, while PBE0 slightly overestimates HONS energy relative to *trans*-HSNO as well as the *cis*-to-*trans* isomerization barrier, both by ~2 kcal/mol.

3.3 SN(H)O, *Y*-isomer

Both pathways of HSNO isomerization into the cyclic structure (Scheme 2) involve the *Y*-isomer SN(H)O which is 4.66 kcal/mol higher in energy relative to *trans*-HSNO at the CCSD(T)/CBS+CORR+ZPE (Table 3). The *Y*-isomer is also planar, with the S–N bond ~0.2 Å shorter compared to *trans*-HSNO (1.624 vs 1.858Å, Table 3). The calculated SN(H)O properties converge rather fast with the basis set size, and the

Physical Chemistry Chemical Physics Accepted Manuscript

This journal is © the Owner Societies 2014

inclusion of quadruple excitations has a relatively small effect on the geometry and the energetic properties of SN(H)O.

Table 3 Geometric parameters of the *Y*-isomer SN(H)O and the cyclic isomer *cycl*-SONH, and their energy relative to *trans*-HSNO (ΔE, kcal/mol) calculated at different levels of theory.

	Y-isomer SN(H)O						Cyclic isomer *cycl*-SONH					
	S–N/Å	N–O/Å	S–O/Å	N–H/Å	SNO/°	ΔE	S–N/Å	N–O/Å	S–O/Å	N–H/Å	SNO/°	ΔE
CCSD(T)/												
AVDZ	1.647	1.248	2.619	1.036	129.07	4.48	1.789	1.484	1.744	1.039	63.61	33.75
AVTZ	1.629	1.239	2.597	1.028	129.20	2.21	1.754	1.473	1.702	1.028	62.97	28.39
AVQZ	1.624	1.236	2.588	1.027	129.17	1.81	1.745	1.468	1.694	1.026	62.94	28.09
AV5Z	1.622	1.235	2.585	1.027	129.16	1.77	1.743	1.466	1.691	1.026	62.90	27.80
CBS	1.620	1.234	2.583	1.027	129.159	1.75	1.740	1.465	1.688	1.026	62.87	27.63
CBS_{TQ}	1.620	1.233	2.582	1.027	129.14	1.52	1.739	1.463	1.688	1.025	62.91	27.86
CBS_{Q5sp}						1.73						27.50
ΔQ	0.006	0.003	0.006	0.000	-0.14	0.47	0.003	0.003	0.004	0.001	-0.02	1.21
ΔCV	-0.003	-0.002	-0.005	-0.001	0.00	-0.29	-0.003	-0.003	-0.004	-0.001	-0.04	0.02
ΔSR	0.001	0.000	0.001	0.000	0.01	-0.20	0.002	0.000	0.002	0.000	0.02	-0.14
ΔZPE						2.93						2.22
CBS+CORR	1.624	1.235	2.586	1.026	129.03	1.73	1.742	1.465	1.690	1.026	62.82	28.71
CBS+CORR+ZPE						4.66						30.94
CBS_{TQ}+CORR	1.624	1.233	2.585	1.026	129.02	1.50	1.741	1.464	1.689	1.025	62.87	28.95
CBS_{TQ}+CORR+ZPE						4.43						31.17
CBS_{5sp}+CORR+ZPE						4.67						29.72
PBE0/def2-TZVPPD	1.616	1.216	2.569	1.031	129.75	1.30	1.728	1.438	1.678	1.026	63.25	30.25
PBE0/def2-TZVPPD+ZPE						4.14						32.54
CBS-QB3	1.636	1.223	2.594	1.035	129.65	0.60	1.769	1.448	1.731	1.029	64.19	28.33
CBS-QB3+ZPE						3.45						30.42

Inexpensive CBS_{TQ} extrapolation scheme demonstrates very close result to $CBS_{TQ5/Q5}$, with the maximum difference between extrapolated bond lengths less than 0.002 Å. Again, the results of CBS-QB3 and PBE0 calculations agree well with the high-level coupled-cluster reference data (Table 3).

3.4 Cyclic isomer *cycl*-SONH

CCSD(T) calculations confirm that the three-membered cyclic structure (Figure 2, *cycl*-SONH, Table 3) exists as a local minimum on the potential energy surface. The S–N bond in this molecule, 1.742 Å at the CCSD(T)/CBS+CORR (Table 3), is significantly shorter compared to *trans*-HSNO (1.858 Å), but longer compared to the *Y*-isomer SN(H)O (1.624 Å). The N–O bond in *cycl*-SONH, 1.465Å, is significantly longer compared to *trans*-HSNO (1.180 Å) and the *Y*-isomer (1.235 Å). Inclusion of quadruple excitations does not affect the geometry to the same degree as in the case of HSNO, which suggests a smaller role of multireference effects. Indeed the values of the T_1 and D_1 coupled cluster diagnostics, 0.016 and 0.046, respectively, are below the threshold values established for multi-reference systems, 0.02 and 0.05, respectively. Unlike the other HSNO isomers considered here, the cyclic form *cycl*-SONH is significantly higher in energy, ~31 kcal/mol above *trans*-HSNO, as estimated at the CCSD(T)/CBS+CORR+ZPE level (Table 3). The deviations of the geometric parameters calculated with CBS-QB3 and PBE0 are slightly larger for *cycl*-SONH compared to the other isomers, e.g. the S–N bond length is underes-

Physical Chemistry Chemical Physics Accepted Manuscript

timated by >0.01 Å with PBE0 and overestimated it by ~0.03 Å with CBS-QB3. However, the energy difference relative to *trans*-HSNO (31 kcal/mol) is well reproduced with CBS-QB3 and slightly overestimated by PBE0 (30 and 33 kcal/mol, respectively, Table 3).

3.5 Possible pathways of HSNO isomerization into *cycl*-SONH

The first pathway for the formation of *cycl*-SONH from *trans*-HSNO (Scheme 2A and Figure 2) studied here is an extended version of the reaction scheme proposed by King[17] (Scheme 1A). In order to tautomerize into HOSN, *trans*-HSNO first has to convert into its *cis*-conformer via a small barrier (**TS1**, 8.7 kcal/mol). Then, *cis*-HSNO can isomerize into *cis*-HONS via hydrogen/proton transfer between the sulfur and oxygen atoms, which requires 28.4 kcal/mol to overcome the energy barrier (**TS2**). Next, *cis*-HONS must convert into the *trans*-conformer via 11.7 kcal/mol barrier (**TS3**). However, instead of direct transformation into *cycl*-SONH, *trans*-HONS first converts into the *Y*-isomer SN(H)O via oxygen to nitrogen hydrogen/proton transfer (**TS4**) with a sizable energetic barrier of 45.7 kcal/mol.

Finally, SN(H)O undergoes cyclization into *cycl*-SONH that involves closing of S–N–O angle form ~130° to 63° and pyramidalization at the nitrogen atom through **TS5** associated with a high activation barrier, estimated to be >50 kcal/mol at the CCSD(T)/CBS_{TQ}+CORR+ZPE level.[68] However, a large effect of quadruple excitations on the **TS5** geometry (+0.014 Å) and the corresponding barrier height (-1.8 kcal/mol), as well as large values of T_1 and D_1 diagnostics (0.07 and 0.30, respectively, Table S2) suggests a highly multireference character of the **TS5** structure. Indeed, stability analysis of the corresponding Hartree-Fock wavefunction revealed a significant RHF → UHF instability, with the UHF solution 13.5 kcal/mol lower in energy and the $\langle S^2 \rangle$ value of ~0.9 are indicative of the strongly open-shell character of this TS. Thus, we supplemented the closed-shell coupled-cluster calculations of the SN(H)O cyclization reaction with multireference second-order perturbation theory (CASPT2) calculations that employed (6,6) active space, as described in Computational Details section. The reactions barrier calculated at with CASPT2 is even higher than the CCSD(T) predictions (~58 kcal/mol, Table S3). Improvement of the correlation treatment using single point multireference configuration interaction (MRCI) with Davidson correction (MRCI+Q) calculation slightly decreases the barrier (by ~3 kcal/mol).

Besides the multi-step isomerization *trans*-HSNO in the *Y*-isomer SN(H)O via the tautomer HONS (Scheme 2A), we found that *trans*-HSNO can directly convert into SN(H)O via a hydrogen/proton transfer form sulfur to nitrogen through **TS6** (Scheme 2B). Like a similar oxygen to nitrogen hydrogen/proton migration TS (**TS4**), **TS6** has a highly strained three-membered ring geometry and thus associated with a large barrier height, ~49 kcal/mol (Figure 2). The second and final step in this alternative pathway also involves SN(H)O cyclization into *cycl*-SONH.

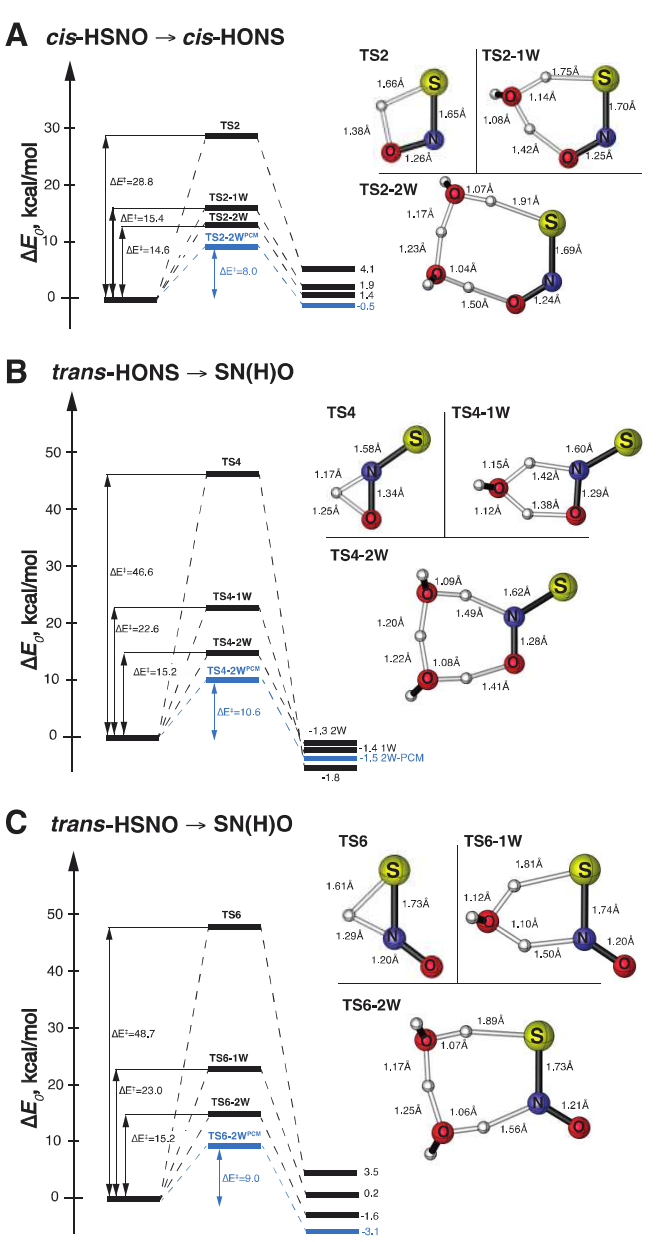

Figure 3 Effect of the aqueous environment on the transformation between HSNO isomers: energetic profiles for 'dry' and water-assisted reactions in the gas phase and in PCM water (for two-water assisted reactions), and the structures of the relevant transition states.

Despite some ambiguity in the calculated reaction barrier for the SN(H)O cyclization step, it is clear that the formation of the cyclic form *cycl*-SONH from HSNO at physiological conditions is highly improbable. Indeed, besides a prohibitively high energetic barrier, >50 kcal/mol, formation of *cycl*-SONH is thermodynamically unfavorable, as it is ≥25 kcal/mol higher in energy compared to HSNO and its other isomers (Figure 2). At the same time, the *Y*-isomer SN(H)O and the tautomer HONS are only 4.6 and 5.6 kcal/mol less stable than HSNO, and thus may be thermodynamically accessible at physiological conditions. Interconversion between these three species requires hydrogen/proton migration reactions with substantial (30-50

Physical Chemistry Chemical Physics Accepted Manuscript

This journal is © the Owner Societies 2014

kcal/mol) energetic barriers. However, in aqueous environment these barriers can be significantly decreased by involvement of water molecules.[69,70] Although calculations of water-assisted isomerization reactions at the CCSD(T)/CBS level are prohibitively expensive at the moment, CBS-QB3 and PBE0 methods provide a viable alternative. Indeed, the barriers for the hydrogen/proton migration reactions (**TS2**, **TS4**, and **TS6**, Figure 2) predicted with CBS-QB3 and PBE0 are within 0.8 and 1.0 kcal/mol, respectively, of the high-level coupled-cluster results (Table S4). Thus, we further apply these methods to investigate water assisted interconversion reactions of HSNO isomers and their possible reactions with H_2S.

3.6 Water-assisted HSNO isomerization reactions

Schematic profiles of the isomerization reactions via water-assisted hydrogen/proton migration and the corresponding transition structures obtained at the CBS-QB3 level are shown in Figure 3. The transition structure for sulfur-to-oxygen migration necessary for *cis*-HSNO→*cis*-HONS transformation,**TS2**, is less strained compared to the other two reactions, and the corresponding reaction barrier is relatively low, ~29 kcal/mol (Figure 3A). Addition of a water molecule relives the strain provides and a proton shuttle in a six-membered ring **TS2-1W**, which lowers the reaction barrier to 15.4 kcal/mol. While addition of the second water molecule leads to 8-member ring **TS2-2W** and has a much weaker effect on the barrier height (14.6 kcal/mol barrier).

The transformation form *trans*-HONS to the *Y*-isomer SN(H)O proceeds via a highly strained three-membered ring transition structure corresponding, **TS4**. Addition of a single water molecule leads to five-membered ring **TS4-1W** and dramatic lowering of the barrier height, from 46.5 to 22.5 kcal/mol (Figure 3B). Addition of the second water molecule leads to even more relaxed 7-member ring **TS4-2W** and further barrier lowering to 15.2 kcal/mol. Much the same way, the water-assisted mechanism decreases the reaction barrier from 48.7 to 15.2 kcal/mol for the direct *trans*-HSNO→SN(H)O transformation that has very similar strained transition structure **TS6** (Figure 3C).

Besides the significant barrier-lowering effect of the addition of water molecules that act as a bridge for a proton transfer, the HSNO isomerization reactions could benefit from the non-specific solvation in highly polar aqueous environment. Indeed, the barrier heights for the reactions assisted by two water molecules calculated using polarizable continuum model (PCM) drop by 4-6 kcal/mol: to 8.0 kcal/mol for *cis*-HSNO→*cis*-HONS transformation, to 10.6 kcal/mol for *trans*-HONS→SN(H)O, and to 9.0 kcal/mol for *trans*-HSNO→SN(H)O transformation (Figure 3). Thus, two of the HSNO isomers, the *Y*-isomer SN(H)O and the tautomer HONS appear to be both thermodynamically and kinetically assessable at physiological conditions.

3.7 Reaction of hydrogen sulfide with *Y*-isomer and *cycl*-SONH

Our calculations suggest that the cyclic form *cycl*-SONH is very unlikely to form at physiological conditions, and thus is a very unlikely source of biological nitroxyl HNO in the reaction with H_2S (Scheme 1B). However, a similar but less strained thus thermodynamically more plausible *Y*-isomer SN(H)O may react with H_2S in a similar way (Scheme 3).

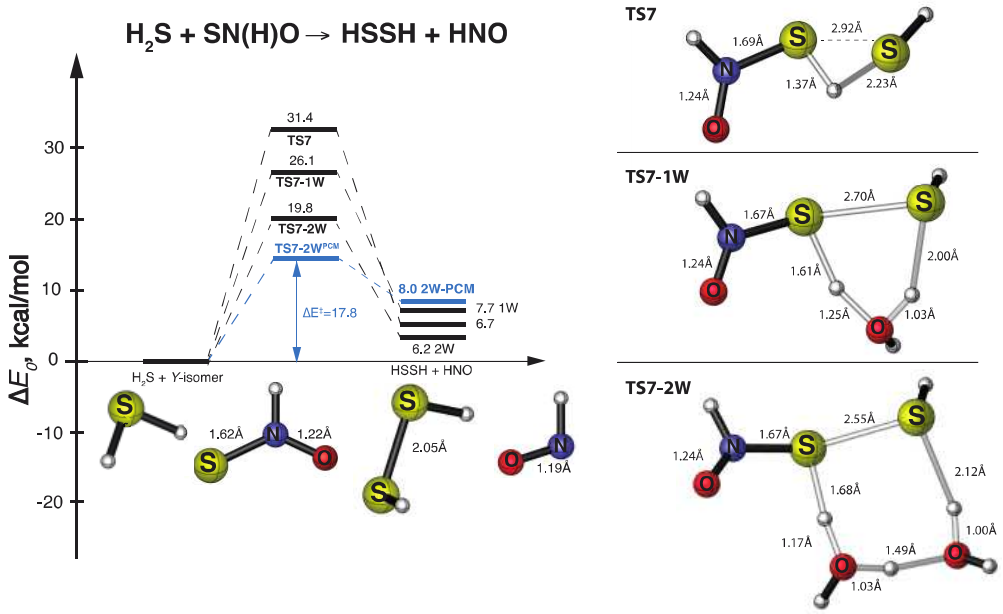

Figure 4 Energetic profiles for 'dry' and water-assisted reactions between the *Y*-isomer SN(H)O and hydrogen sulfide H_2S, and the relevant transition state structures, calculated at the UPBE0/def2-TZVPPD level.

Physical Chemistry Chemical Physics Accepted Manuscript

Scheme 3 Possible reaction of the *Y*-isomer SN(H)O and H_2S; *cf.* Scheme 1B.

Indeed, we were able to locate a transition state for reaction of *Y*-isomer with H_2S, **TS7** (Figure 4). This transition structure corresponds to simultaneous hydrogen/proton transfer between the two sulfur atoms and a covalent bond formation between them. As **TS7** was found to have an open-shell character, we used symmetry-broken unrestricted PBE0 (UPBE0) approach to study this reaction that is expected to be more robust in this situation. Similarly to the isomerization reactions (Figures 2 and 3), water-assisted proton shuffle significantly decreases the reaction barrier, from 31.4 kcal/mol to 26.1 and 19.8 kcal/mol for one- and two-water assisted reactions (**TS7-1W** and **TS7-2W**, Figure 4). At the same time, addition of water molecules decreases the open-shell character of the transition structure: $\langle S^2 \rangle$ = 0.5 for the 'dry' **TS7**, while it drops to 0.2 and 0.1 for **TS7-1W** and **TS7-2W**, respectively.[71] Transition into polarizable aqueous environment modeled with PCM approach further decreases the barrier height to 17.8 kcal/mol for two-water assisted reaction (**TS7-2W**^{PCM}, Figure 4).

For completeness, we also investigated the reaction of *cycl*-SONH with H_2S proposed in the literature[17] (Scheme 1B). The energetic barrier for this reaction (~30 kcal/mol, Figure 5) is associated with the transition structure **TS8** that corresponds to simultaneous sulfur-sulfur bond formation and hydrogen atom exchange, which is similar to the TS of the SN(H)O + H_2S reaction (**TS7**, Figure 4). Curiously, CCSD(T), CBS-QB3, as well as PBE0 calculations suggest that **TS8** does not directly lead to the products—HSSH and HNO—but rather leads to an unusual intermediate structure HSS(H)ONH that preserves the initial SNO three-membered ring (Figure 5),[72] and features a hypervalent sulfur atom simultaneously connected to the H, O, and N atoms, as well to the other S atom.[73] Decomposition of the HSS(H)ONH intermediate by breaking the S–O and S–N bonds (**TS9**, Figure 5) is associated with a small (~7 kcal/mol) energetic barrier. Although the reaction of *cycl*-SONH with H_2S is rather unlikely to have biochemical relevance, its unusual mechanism revealed by our calculations illustrates and underscores the richness of the chemistry of sulfur-nitrogen species.

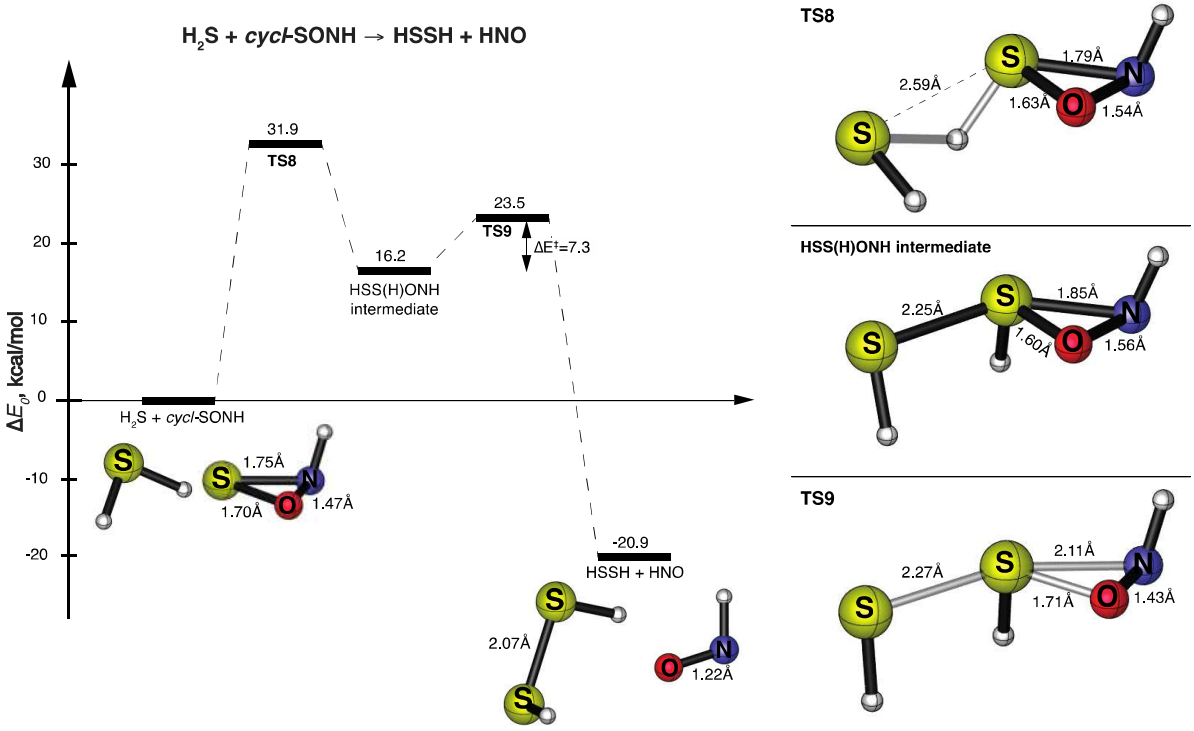

Figure 5 Energetic profile for the proposed (Scheme 1B) reaction between the cyclic isomer *cycl*-SONH and reaction H_2S and the structures of relevant transition states and the HSS(H)ONH intermediate, calculated at the CCSD(T)/AVTZ+ZPE level.

Physical Chemistry Chemical Physics Accepted Manuscript

This journal is © the Owner Societies 2014

4. Conclusions

Recent discoveries of the potential biological relevance of the smallest *S*-nitrorsothiol—HSNO—opened up numerous possibilities of the secondary biochemical processes involving this molecule, including formation of derivative species, including—but certainly not limited to—SNO^- and $SSNO^-$ anions and HSNO isomers. In this computational study, we revisited the possible pathways of HSNO isomerization at physiological conditions and tested a recent hypothesis[17] on the possibility of HSNO transformation into its cyclic isomer *cycl*-SONH. Our calculations suggest that while formation of this cyclic structure is not feasible thermodynamically as well as kinetically, formation of the tautomeric form HONS and the *Y*-isomer SN(H)O via water-assisted proton transfer reactions is not at all impossible in the physiological, aqueous environment. These two HSNO isomers then may engage in a variety of reactions with other molecules present in biological milieu. In fact, while the proposed[17] formation of nitroxyl HNO in the reaction of H_2S with the cyclic form is unlikely, possibility of a reaction between H_2S and the *Y*-isomer SN(H)O leading to HSSH and HNO cannot be excluded. Further studies of the reactions involving HSNO and its derivative species will be required to reveal the entire spectrum of possible reactions that can tie together the biological signaling pathways the two gasotransmitters, NO and H_2S.

Methodologically, this work once again highlighted the complex and unusual electronic structure of the –SNO group: compared to its isomers, the computed properties of HSNO demonstrate the slowest convergence with respect to the electron correlation treatment and the basis set size. Therefore, computational methods used to study the HSNO/RSNO reactions should be always carefully benchmarked and validated against high-level *ab inito* results.

Acknowledgements

This work was supported by the National Science Foundation (NSF) CAREER award CHE–1255641. Calculations were performed on the high-performance computing cluster *Père* at Marquette University funded by NSF awards OCI–0923037 and CBET–0521602. Q.K.T. thanks Prof. S. Bruce King (Wake Forest University) for fruitful discussions; B.J.A. and Q.K.T. thank Prof. Alex Blom (Alverno College) for assistance with organizing B.A.'s internship at Marquette University.

Notes and references

[a] Department of Chemistry, Marquette University, P.O. Box 1881, Milwaukee, WI 53201-1881, United States.
[b] Alverno College, P.O. Box 343922, Milwaukee, WI 53234-3922, United States.

Electronic Supplementary Information (ESI) available: [Supplementary Tables S1–S8, Supplementary Figures S1-S2, Cartesian coordinates and energies for all calculated structures]. See DOI: 10.1039/b000000x/

1 B. C. Smith and M. A. Marletta, *Curr. Opin. Chem. Biol.*, 2012, **16**, 498-506.
2 K. A. Broniowska and N. Hogg, *Antioxid. Redox. Signal.*, 2012, **17**, 969-980.
3 W. H. Koppenol, *Inorg. Chem.*, 2012, **51**, 5637-5641.
4 D. T. Hess, A. Matsumoto, S. -O. Kim, H. E. Marshall, and J. S. Stamler, *Nat. Rev. Mol. Cell. Biol.*, 2005, **6**, 150-166.
5 D. L. H. Williams, *Acc. Chem. Res.*, 1999, **32**, 869-876.
6 T. A. Heinrich, R. S. da Silva, K. M. Miranda, C. H. Switzer, D. A. Wink, and J. M. Fukuto, *Br. J. Pharmacol.*, 2013, **169**, 1417-1429.
7 C. E. Paulsen and K. S. Carroll, *Chem. Rev.*, 2013, **113**, 4633-4679.
8 M. D. Bartberger, K. N. Houk, S. C. Powell, J. D. Mannion, K. Y. Lo, J. S. Stamler, and E. J. Toone, *J. Am. Chem. Soc.*, 2000, **122**, 5889-5890.
9 P. O. Tchir and R. D. Spratley, *Can. J. Chem.*, 1975, **53**, 2318-2330.
10 P. O. Tchir and R. D. Spratley, *Can. J. Chem.*, 1975, **53**, 2331-2336.
11 R. P. Müller, M. Nonella, P. Russegger, and J. R. Huber, *Chem. Phys.*, 1984, **87**, 351-361.
12 M. Nonella, J. R. Huber, and T. K. Ha, *J. Phys. Chem.*, 1987, **91**, 5203-5209.
13 Q. Li and J. R. Lancaster, *Nitric Oxide*, 2013, **35**, 21-34.
14 J. L. Miljkovic, I. Kenkel, I. Ivanović-Burmazović, and M. R. Filipovic, *Angew. Chem. Int. Ed. Engl.*, 2013,
15 M. R. Filipovic, J. L. Miljkovic, T. Nauser, M. Royzen, K. Klos, T. Shubina, W. H. Koppenol, S. J. Lippard, and I. Ivanović-Burmazović, *J. Am. Chem. Soc.*, 2012, **134**, 12016-12027.
16 M. R. Filipovic, M. Eberhardt, V. Prokopovic, A. Mijuskovic, Z. Orescanin-Dusic, P. Reeh, and I. Ivanovic-Burmazovic, *J. Med. Chem.*, 2013, **56**, 1499-1508.
17 S. B. King, *Free. Radic. Biol. Med.*, 2013, **55**, 1-7.
18 M. Whiteman, L. Li, I. Kostetski, S. H. Chu, J. L. Siau, M. Bhatia, and P. K. Moore, *Biochem. Biophys. Res. Commun.*, 2006, **343**, 303-310.
19 M. M. Cortese-Krott, B. O. Fernandez, J. L. Santos, E. Mergia, M. Grman, P. Nagy, M. Kelm, A. Butler, and M. Feelisch, *Redox. Biology.*, 2014, 10.1016/j.redox.2013.12.031
20 J. M. Fukuto, A. S. Dutton, and K. N. Houk, *Chembiochem*, 2005, **6**, 612-619.
21 K. M. Miranda, *Coord. Chem. Rev.*, 2005, **249**, 433-455.
22 J. M. Fukuto, C. J. Cisneros, and R. L. Kinkade, *J. Inorg. Biochem.*, 2013, **118**, 201-208.
23 C. Baciu and J. W. Gauld, *J. Phys. Chem. A*, 2003, **107**, 9946-9952.
24 Q. K. Timerghazin, G. H. Peslherbe, and A. M. English, *Phys. Chem. Chem. Phys.*, 2008, **10**, 1532-1539.
25 M. Hochlaf, R. Linguerri, and J. S. Francisco, *J. Chem. Phys.*, 2013, **139**, 234304.
26 Q. K. Timerghazin, A. M. English, and G. H. Peslherbe, *Chem. Phys. Lett.*, 2008, **454**, 24-29.
27 C. Yu-Juan, Y. Hai-Tao, F. Hong-Gang, X. Bai-Fu, L. Ze-Sheng, and S. Jia-Zhong, *Chin. J. Chem.*, 2003, **21**, 30-35.
28 V. Ruangpornvisuti, *Int. J. Quantum Chem.*, 2009, **109**, 275-284.
29 C. -H. Lai, E. Y. Li, and P. -T. Chou, *Theor. Chem. Acc.*, 2007, **117**, 145-152.
30 H.-J. Werner, P. J. Knowles, G. Knizia, F. R. Manby, M. Schütz, P. Celani, T. Korona, R. Lindh, A. Mitrushenkov, G. Rauhut, K. R. Shamasundar, T. B. Adler, R. D. Amos, A. Bernhardsson, A.

Physical Chemistry Chemical Physics Accepted Manuscript

Berning, D. L. Cooper, M. J. O. Deegan, A. J. Dobbyn, F. Eckert, E. Goll, C. Hampel, A. Hesselmann, G. Hetzer, T. Hrenar, G. Jansen, C. Köppl, Y. Liu, A. W. Lloyd, R. A. Mata, A. J. May, S. J. McNicholas, W. Meyer, M. E. Mura, A. Nicklass, D. P. O'Neill, P. Palmieri, K. Pflüger, R. Pitzer, M. Reiher, T. Shiozaki, H. Stoll, A. J. Stone, R. Tarroni, T. Thorsteinsson, M. Wang, and A. Wolf, *MOLPRO, version 2010.1, a package of ab initio programs,* see http://www.molpro.net

31 T. D. Crawford and H. F. Schaefer, *Rev. Comput. Chem.*, 2000, **14**, 33-136.

32 K. Raghavachari, G. W. Trucks, J. A. Pople, and M. Head-Gordon, *Chem. Phys. Lett.*, 1989, **157**, 479-483.

33 Y. J. Bomble, J. F. Stanton, M. Kállay, and J. Gauss, *J. Chem. Phys.*, 2005, **123**, 054101.

34 M. Kállay, *MRCC, a string-based quantum chemical program suite*, see http://tc03.fkt.bme.hu

35 J.F. Stanton, J. Gauss, M.E. Harding, P.G. Szalay with contributions from A.A. Auer, R.J. Bartlett, U. Benedikt, C. Berger, D.E. Bernholdt, Y.J. Bomble, L. Cheng, O. Christiansen, M. Heckert, O. Heun, C. Huber, T.-C. Jagau, D. Jonsson, J. Jusélius, K. Klein, W.J. Lauderdale, D.A. Matthews, T. Metzroth, L.A. Mück, D.P. O'Neill, D.R. Price, E. Prochnow, C. Puzzarini, K. Ruud, F. Schiffmann, W. Schwalbach, S. Stopkowicz, A. Tajti, J. Vázquez, F. Wang, J.D. Watts and the integral packages MOLECULE (J. Almlöf and P.R. Taylor), PROPS (P.R. Taylor), ABACUS (T. Helgaker, H.J. Aa. Jensen, P. Jørgensen, and J. Olsen), and ECP routines by A. V. Mitin and C. van Wüllen, *CFOUR, a quantum chemical program package,* see http://www.cfour.de

36 T. J. Lee and P. R. Taylor, *Int. J. Quantum Chem.*, 1989, **36**, 199-207.

37 C. L. Janssen and I. Nielsen, *Chem. Phys. Lett.*, 1998, **290**, 423-430.

38 J. Kästner, J. M. Carr, T. W. Keal, W. Thiel, A. Wander, and P. Sherwood, *J. Phys. Chem. A.*, 2009, **113**, 11856-11865.

39 D. C. Liu and J. Nocedal, *Math. Program.*, 1989, **45**, 503-528.

40 J. Nocedal, *Math. Comp.*, 1980, **35**, 773-782.

41 C. J. Cerjan and W. H. Miller, *J. Chem. Phys.*, 1981, **75**, 2800.

42 J. Simons, P. Joergensen, H. Taylor, and J. Ozment, *J. Phys. Chem.*, 1983, **87**, 2745-2753.

43 J. Baker, *J. Comput. Chem.*, 1986, **7**, 385-395.

44 A. Banerjee, N. Adams, J. Simons, and R. Shepard, *J. Phys. Chem.*, 1985, **89**, 52-57.

45 S. R. Billeter, A. J. Turner, and W. Thiel, *Phys. Chem. Chem. Phys.*, 2000, **2**, 2177-2186.

46 T. H. Dunning Jr, *J. Chem. Phys.*, 1989, **90**, 1007.

47 T. H. Dunning Jr, K. A. Peterson, and A. K. Wilson, *J. Chem. Phys.*, 2001, **114**, 9244.

48 T. Helgaker, W. Klopper, H. Koch, and J. Noga, *J. Chem. Phys.*, 1997, **106**, 9639.

49 D. Feller and K. A. Peterson, *J. Chem. Phys.*, 1999, **110**, 8384.

50 K. A. Peterson, D. E. Woon, and T. H. Dunning Jr, *J. Chem. Phys.*, 1994, **100**, 7410.

51 M. Douglas and N. M. Kroll, *Ann. Phys.*, 1974, **82**, 89-155.

52 G. Jansen and B. A. Hess, *Phys. Rev. A.*, 1989, **39**, 6016-6017.

53 K. A. Peterson and T. H. Dunning Jr, *J. Chem. Phys.*, 2002, **117**, 10548.

54 H. -J. Werner, *Mol. Phys.*, 1996, **89**, 645-661.

55 H. -J. Werner and P. J. Knowles, *J. Chem. Phys.*, 1985, **82**, 5053.

56 P. J. Knowles and H. -J. Werner, *Chem. Phys. Lett.*, 1985, **115**, 259-267.

57 P. Celani and H. -J. Werner, *J. Chem. Phys.*, 2003, **119**, 5044.

58 S. R. Langhoff and E. R. Davidson, *Int. J. Quantum Chem.*, 1974, **8**, 61-72.

59 C. Adamo and V. Barone, *J. Chem. Phys.*, 1999, **110**, 6158.

60 J. P. Perdew, K. Burke, and M. Ernzerhof, *Phys. Rev. Lett.*, 1996, **77**, 3865.

61 J. A. Montgomery Jr, M. J. Frisch, J. W. Ochterski, and G. A. Petersson, *J. Chem. Phys.*, 2000, **112**, 6532.

62 M. J. Frisch, G. W. Trucks, H. B. Schlegel, G. E. Scuseria, M. A. Robb, J. R. Cheeseman, G. Scalmani, V. Barone, B. Mennucci, G. A. Petersson, H. Nakatsuji, M. Caricato, X. Li, H. P. Hratchian, A. F. Izmaylov, J. Bloino, G. Zheng, J. L. Sonnenberg, M. Hada, M. Ehara, K. Toyota, R. Fukuda, J. Hasegawa, M. Ishida, T. Nakajima, Y. Honda, O. Kitao, H. Nakai, T. Vreven, J. A. Montgomery, Jr., J. E. Peralta, F. Ogliaro, M. Bearpark, J. J. Heyd, E. Brothers, K. N. Kudin, V. N. Staroverov, R. Kobayashi, J. Normand, K. Raghavachari, A. Rendell, J. C. Burant, S. S. Iyengar, J. Tomasi, M. Cossi, N. Rega, J. M. Millam, M. Klene, J. E. Knox, J. B. Cross, V. Bakken, C. Adamo, J. Jaramillo, R. Gomperts, R. E. Stratmann, O. Yazyev, A. J. Austin, R. Cammi, C. Pomelli, J. W. Ochterski, R. L. Martin, K. Morokuma, V. G. Zakrzewski, G. A. Voth, P. Salvador, J. J. Dannenberg, S. Dapprich, A. D. Daniels, Ö. Farkas, J. B. Foresman, J. V. Ortiz, J. Cioslowski, and D. J. Fox, *Gaussian 09, Revision C.01*, see http://www.gaussian.com

63 D. Rappoport and F. Furche, *J. Chem. Phys.*, 2010, **133**, 134105.

64 F. Weigend and R. Ahlrichs, *Phys. Chem. Chem. Phys.*, 2005, **7**, 3297-3305.

65 H. P. Hratchian and H. B. Schlegel, *J. Chem. Phys.*, 2004, **120**, 9918-9924.

66 H. P. Hratchian and H. B. Schlegel, *J. Chem. Theory and Comput.*, 2005, **1**, 61-69.

67 E. Cances, B. Mennucci, and J. Tomasi, *J. Chem. Phys.*, 1997, **107**, 3032.

68 Although the barrier height for SN(H)O cyclization into *cycl*-SONH increases with the basis set size, CCSD(T)/AV5Z single-point energy for the CCSD(T)/AVQZ geometry gives a lower barrier than CCSD(T)/AVQZ, Table S4. As a reslult, CBS_{Q5sp} scheme highly underestimates the barrier height—43.9 kcal/mol; therefore CBS_{TQ} extrapolation was used to estimate the barrier height.

69 Z. Wu, F. Ban, and R. J. Boyd, *J. Am. Chem. Soc.*, 2003, **125**, 6994-7000.

70 E. V. Ivanova and H. M. Muchall, *J. Phys. Chem. A.*, 2007, **111**, 10824-10833.

71 The corresponding differences between the closed shell (RPBE0) and open-shell (UPBE0) energies are 2.6, 0.3, and 0.2 kcal/mol for **TS7**, **TS7-1W**, and **TS7-2W**, respectively.

72 Coupled-cluster and T_1 and D_1 diagnostics (Table S5 in Supporting Information) as well as the wavefunction stability tests do not suggest significant multi-reference or open shell character for HSS(H)ONH intermediate.

73 Natural Bond Orbital (NBO) analyses suggest that the in-ring sulfur atom is indeed hypervalent as its □-bonds to N and S atoms involve $sp^{20}d^{11}$ and $sp^{11}d^{9}$ hybridized orbitals, respectively. This makes the HSS(H)ONH intermediate very unusual, as the hypervalent com-

Physical Chemistry Chemical Physics Accepted Manuscript

This journal is © the Owner Societies 2014

pounds of sulfur and other elements usually do not make use of sp^yd^z hybrids and conform the octet rule: e.g., F. Weinhold and C. R. Landis, *Valency and Bonding: A Natural Bond Orbital Donor-Acceptor Perspective*, Cambridge University Press, New York, 2003.

TOC Absract

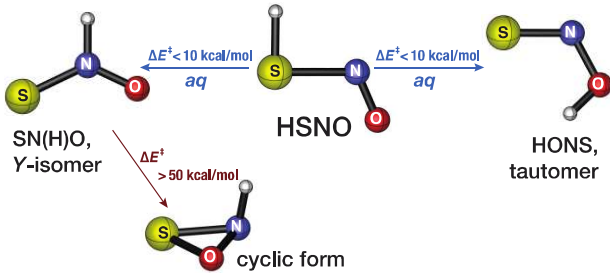

We computationally demonstrate that thionitrous acid HSNO, putatively an important biological signalling molecule, may convert—at physiological conditions—to other isomeric forms that may potentially have their own biological activity.

Physical Chemistry Chemical Physics Accepted Manuscript

TOC Absract

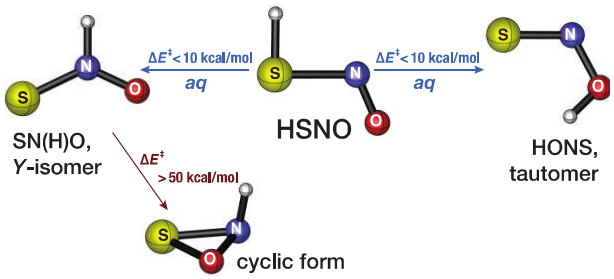

We computationally demonstrate that thionitrous acid HSNO, putatively an important biological signalling molecule, may convert—at physiological conditions—to other isomeric forms that may potentially have their own biological activity.

Physical Chemistry Chemical Physics Accepted Manuscript